RESEARCH PAPER

The onset of Casson fluid convection in a permeable medium layer produced by purely inner heating with magnetic field

Dhananjay Yadav [a, *], Mukesh Kumar Awasthi [b], A. M. Mohamad [a], Ravi Ragoju [c], Krishnendu Bhattacharyya [d], Mohammad Hassan[e]

[a] *Department of Mathematical & Physical Sciences, University of Nizwa, Nizwa, P.O.B.-616, Oman*
[b] *Department of Mathematics, Babasaheb Bhimrao Ambedkar University, Lucknow 226025, India*
[c] *Department of Applied Sciences, National Institute of Technology Goa, Goa 403401, India*
[d] *Department of Mathematics, Institute of Science, Banaras Hindu University,Varanasi–221005, Uttar Pradesh, India*
[e] *Department of Mathematics, North Eastern Regional Institute of Science and Technology, Itanagar, Arunachal Pradesh, 791109, India*

Abstract

In this inspection, the control of the magnetic power on the onset of Casson fluid convection formed by purely inner warming in a porous medium layer is examined. The modified Darcy model is employed to designate the rheological arrival of Casson liquid flow in a porous matrix. Two types of thermal boundaries are exploited, namely, type (I) both isothermal and type (II) lower insulated and top isothermal boundaries. Using the linear stability inspection and Galerkin technique, the approximate analytical solution and numerical solution correct to one decimal place are offered. It is detected that for type (I) boundary conditions, the convective wave concentrates in the upper layer if it occurs, whereas for type (II) boundary conditions, it emphases in the whole layer. The magnetic Chandrasekhar number postpones the convection movement while the Casson constraint accelerates it. The facet of the convective cells drops with enhancing the magnetic strength and the Casson constraint. In the absenteeism of magnetic field, the Casson constraint has no regulation on the dimension of convective cells. It is also found that the presented analytical result with two term Galerkin process has overall 5% error, while with one term Galerkin process the error was overall 19%.

Keywords: Casson fluid; Convective motion; Magnetic field; Porous medium; Internal Rayleigh number;

1. Introduction

Internally warmth convective flow, in which the flow of a liquid is motivated by buoyancy force produced by inner causes of heat, is detected in an extensive range of natural and engineering environments, and exhibits a vital role in many areas for example geophysics, astrophysics, metal casting, pharmacological, chemical and cosmetic industries. For in case, convection in the Earth's mantle engendered by radioactive deterioration, which in turn impacts on plate tectonics and the planet's magnetic force and convection in porous layer generated by own heat source of porous material [1-4]. Consequently, the role of interior heat generation becomes very significant in

numerous such applications. Gasser and Kazimi [5] examined the convection in a permeable medium layer engendered by interior heat production and derived the conditions for the beginning of convective drive in term of the critical internal Rayleigh number. The weight of rotation and Darcy number on the arrival of convective wave persuaded by only inner heating in a permeable matrix was inspected by Yadav et al. [6]. They established that the result of growing rotation parameter constrains the start of convection, whereas Darcy number displays dual behaviour. The addition with nanofluid is also finished by Yadav et al. [7]. Mahajan et al. [8] inspected the penetrative convective movement caused by only interior warming in a flat ferrofluid saturated porous layer by taking four diverse kinds of heat resource functions. The influence of steady interior warmth source and changeable descendent gravity power on the arrival of convective drive in an anisotropic permeable matrix was examined by Yadav [9]. He found that both the heat anisotropy constraint and gravity disparity constraint postponed the start of convection. Recently, Jain and Solomatov[10] examined the effect of viscosity on the onset of convection in inner heated fluids and derived the asymptotic scaling relations for the critical Rayleigh number and other parameters. The more works with inner heating effects were made by Akbarzadeh [11], Capone et al. [12], Gaikwad and Kouser [13], and Nield and Kuznetsov [14].

In the past few years, non-Newtonian fluids have worldwide utilizations in science and engineering such as processing and mining industries, petroleum production and pharmacological, chemical and cosmetic industries. The Casson model is a non-Newtonian model and well determines the shear thinning consequences [15-20]. The blood, ink and molten chocolate are commonly categorized to Casson materials. Aghighi et al. [21] analysed the convective flow in a Casson fluid and detected that the yield stress has a stabilizing consequence by declining the convection asset. Devi et al. [22] inspected the heat source impact on the thermosalinity motion of Casson nanofluids and detected that the Casson factor accelerates the convection. Qadan et al. [23] analysed the mixed convective boundary layer movement on a flat circular cylinder engrossed in a Casson liquid and they noticed that the temperature profile declines as surge the Casson parameter. Reddy et al. [24] calculated the thermohaline convective flow of a Casson liquid in a permeable layer and established that the Casson element weakens the movement. Lately, Yadav et al. [25] examined the chemical reaction outcome on the thermohaline Casson liquid convective drive in a permeable layer. They identified that the over stable nature of convective measure arises only if the valuation of the solutal Rayleigh-Darcy number is smaller than zero.

The outcome of magnetic power can postponement or can advance the arrival of convective drive. The magnetic field in an arrangement of electrically conducting fluids generates the Lorentz force and this force disturbs the convection pointedly. Rudraiah and Vortmeyer [26] examined the value of magnetic forte on the convective motions of a conducting fluid in a porous bed. They created that the magnetic arena postpones the convective drive. Abd-el-Malek and Helal [27] calculated the time dependent laminar flow subjected to a magnetic field. They instituted that the velocity edge-layer wideness converts lesser for the upsurge in the magnetic effect number. Recently, Devi and Gupta [28] examined the Casson nanofluid movement problem in the occurrence of upright magnetic force, heated from bottom. They found that the Chandrasekhar number affects the critical wave number largely whereas the Casson factor affects it slightly. Some other examinations on convective motion with numerous diverse conditions were accomplished by Mahajan and Sharma [29], Sheikholeslami [30], Deepika et al. [31] and Umavathi et al. [32].

The literature review demonstrates that no examination has been established in the literature which studies the effect of magnetic power on the convective flow caused by purely inner heating in a regular fluid or a non-Newtonian Casson fluid. Owing to the potential applications, the intention of the present work is to inspect the influence of magnetic power on the onset of Casson fluid convective movement produced by purely inner warming in a porous matrix. Utilizing the linear stability standard, the purebred equations are produced and assessed analytically as well as numerically by operating the progressive order Galerkin procedure.

2. Problem statement

Let us consider a Casson fluid convection, formed by purely inner warming of power S_0, in a flat porous layer restricted among two planes at $z = 0$ and $z = H$ as shown in Fig.1. It is estimated that a continuous magnetic field $\mathbf{F} = (0, 0, F_0)$ is executed to the flow. On using the Casson fluid form of Darcy's rule as executed by Shuaib et al. [33], Khan et al. [34] and Makinde and Reddy [18], the suitable leading equations subjected to this model are [25] :

$$\nabla \cdot \mathbf{v}_D = 0, \tag{1}$$

$$\left(1+\frac{1}{\eta}\right)\frac{\mu_\eta}{K}\,\mathbf{v}_D = -\nabla P + m_F\,(\mathbf{F}\cdot\nabla)\mathbf{F} + \rho_0\left[1-\alpha_\theta\left(\theta-\theta_0\right)\right]\mathbf{g}, \tag{2}$$

$$\left[(\rho c)_s\frac{\partial}{\partial\tau} + (\rho c)(\mathbf{v}_D.\nabla)\right]\theta = k_s\nabla^2\theta + S_0, \tag{3}$$

$$\left[\frac{\partial}{\partial\tau}+(\mathbf{v}_D\cdot\nabla)\right]\mathbf{F} = \frac{m_F}{\rho_0}\nabla^2\mathbf{F} + (\mathbf{F}\cdot\nabla)\mathbf{v}_D, \tag{4}$$
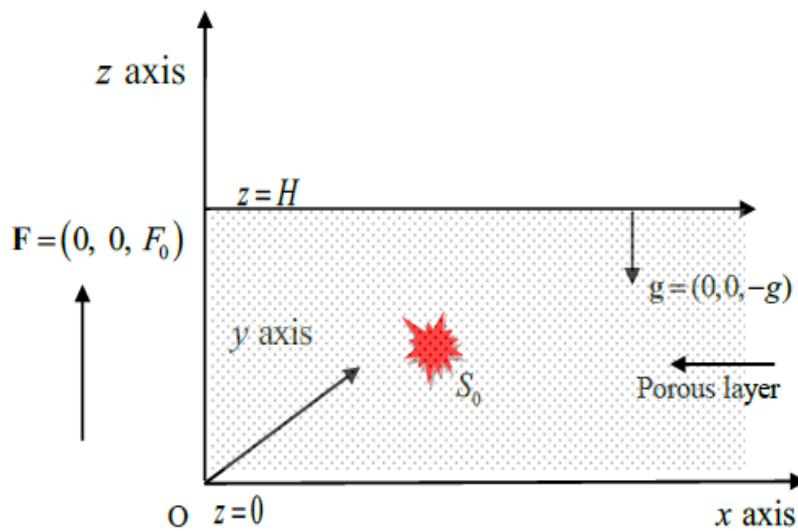
$$\nabla\cdot\mathbf{F}=0 \tag{5}$$

Fig. 1: Graphic depiction of the considered problem.

Here, $\mathbf{v}_D\left(u_D, v_D, w_D\right)$ signifies the Darcy's velocity of the Casson fluid, $\mathbf{g}$ displays the gravity acceleration, θ shows the temperature, τ indicates time, ρ_0 wealth the basic density at $\theta = \theta_0$, P shows the pressure, α_θ is the warmth extension extent, k_s displays for the warmth conductivity, K means the permeability, m_F expresses the magnetic permeability of the Casson liquid, (ρc) and $(\rho c)_s$ appearance for the thermal capacities of Casson liquid and effectually porous matrix, η is the Casson constraint and μ_η terms the plastic dynamic viscosity of the Casson liquid. Two types of boundary specious are taken as [7, 35]:
Type (I) both boundaries' isothermals

$$w_D = 0, \ \theta = \theta_0 \quad \text{at } z = 0, H \tag{6a}$$

Type (II) lower insulated and upper isothermal

$$w_D = 0, \ \partial\theta/\partial z = 0 \ \text{ at } z = 0 \tag{6b}$$
$$w_D = 0, \ \theta = \theta_0 \qquad \text{at } z = H.$$

Now, the following non-dimensional variables are introduced as:

$$\hat{\mathbf{x}} = \frac{\mathbf{x}}{H}, \ \hat{\mathbf{v}}_D = \frac{H}{\beta_s}\hat{\mathbf{v}}_D, \ \hat{\tau} = \frac{\tau\beta_s(\rho c)}{H^2(\rho c)_s}, \ \hat{\theta} = \frac{\rho_0 g\alpha_\theta(\theta-\theta_0)KH}{\mu_\eta\beta_s}, \ \hat{\mathbf{F}} = \frac{\mathbf{F}}{F_0}, \ \hat{P} = \frac{PK}{\mu_\eta\beta_s}. \tag{7}$$

Here $\beta_s = k_s/(\rho c)$. Hence, Eqs. (1)-(6) are transformed to dimensionless arrangement as:

$$\hat{\nabla}\cdot\hat{\mathbf{v}}_D = 0, \tag{8}$$

$$\left(1+\frac{1}{\eta}\right)\hat{\mathbf{v}}_D = -\hat{\nabla}\left(\hat{P}+\hat{z}R_D\right)+\hat{\theta}\hat{\mathbf{e}}_{\mathbf{z}}+\mathrm{P_F}\mathrm{Q}_F(\hat{\mathbf{F}}\cdot\hat{\nabla})\hat{\mathbf{F}}, \tag{9}$$

$$\frac{\partial\hat{\theta}}{\partial\hat{\tau}}+\left(\hat{\mathbf{v}}_D\cdot\hat{\nabla}\right)\hat{\theta} = \hat{\nabla}^2\hat{\theta}+R_I \tag{10}$$

$$\left[\frac{1}{\sigma}\frac{\partial}{\partial\hat{\tau}}+\left(\hat{\mathbf{v}}_D\cdot\hat{\nabla}\right)\right]\hat{\mathbf{F}} = \mathrm{P_F}\hat{\nabla}^2\hat{\mathbf{F}}+\left(\hat{\mathbf{F}}\cdot\hat{\nabla}\right)\hat{\mathbf{v}}_D, \tag{11}$$

,

$$\hat{\nabla}\cdot\hat{\mathbf{F}} = \mathbf{0} \tag{12}$$

Type (I) both boundaries' isothermals
$$\hat{w}_D = 0, \ \hat{\theta} = 0 \quad \text{at } \hat{z} = 0,1 \tag{13a}$$

Type (II) lower insulated and upper isothermal
$$\hat{w}_D = 0, \ \partial\hat{\theta}/\partial\tilde{z} = 0 \ \text{ at } \hat{z} = 0 \tag{13b}$$
$$\hat{w}_D = 0, \ \hat{\theta} = 0 \qquad \text{at } \hat{z} = 1.$$

Here, $\sigma = \dfrac{(\rho c)_s}{(\rho c)}$ defines the heat capacities ratio, $\mathrm{R_D} = \dfrac{\rho_0\, g\, KH}{\mu_\eta\beta_s}$ defines the density Rayleigh number,

$\mathrm{R_I} = \dfrac{gKH^3 S_0\rho_0\alpha_\theta}{\mu_\eta k_s\beta_s}$ defines the internal Rayleigh number, $\mathrm{P_F} = \dfrac{m_F}{\rho_0\beta_s}$ defines the magnetic Prandtl number and

$\mathrm{Q_F} = \dfrac{\rho_0 F_0^{\,2} K}{\mu_\eta}$ defines the magnetic Chandrasekhar number.

The basic state of the framework is supposed as:

$$\widehat{\mathbf{v}}_{D,b} = (0,0,0), \ \widehat{\mathbf{F}}_b = \hat{\mathbf{e}}_z, \ \widehat{\theta}_b = \widehat{\theta}_b(\widehat{z}) \tag{14}$$

Thus Eq. (10) gives the gradient of basis state temperature distribution as:

$$\frac{d\widehat{\theta}_b}{d\widehat{z}} = -\frac{R_I}{2}(2\widehat{z} - \psi) \tag{15}$$

Here the assessment of ψ is one for type (I) and zero for type (II) boundary conditions. Eqs. (15) is the same as found by Hamabata and Takashima [35].

3. Perturbed equations

Assuming that the basic flow is triggered to some degree so that the variables adapted as:

$$\widehat{\mathbf{v}}_D = \widehat{\mathbf{v}}_b + \Xi \mathbf{v}_D', \ \tilde{P} = \tilde{P}_b + \Xi P', \widehat{\theta} = \widehat{\theta}_b + \Xi \theta', \widehat{\mathbf{F}} = \hat{\mathbf{e}}_z + \Xi \mathbf{F}'. \tag{16}$$

where Ξ is a minor dimensionless amplitude characteristic. On using the Eq. (16) into Eqs. (8)–(13) and considering $O(\Xi)$, the perturbed equations can be written as:

$$\widehat{\nabla} \cdot \mathbf{v}_D' = 0, \tag{17}$$

$$\left(1 + \frac{1}{\eta}\right)\mathbf{v}_D' = -\widehat{\nabla}P' + \theta'\hat{\mathbf{e}}_z + \mathrm{P}_F\mathrm{Q}_F\frac{\partial \mathbf{F}'}{\partial \widehat{z}}, \tag{18}$$

$$\frac{\partial \theta'}{\partial \widehat{\tau}} - \frac{w_D'R_I}{2}(2\widehat{z} - \psi) - \widehat{\nabla}^2\theta' = 0 \tag{19}$$

$$\frac{\partial \mathbf{F}'}{\partial \widehat{\tau}} = \mathrm{P}_F\widehat{\nabla}^2\mathbf{F}' + \frac{\partial \mathbf{v}_D'}{\partial \widehat{z}}, \tag{20}$$

$$\widehat{\nabla} \cdot \mathbf{F}' = 0 \tag{21}$$

On Eradicating P' and F_z' by taking $\hat{\mathbf{e}}_z \cdot \widehat{\nabla} \times \widehat{\nabla} \times$ on Eq. (18) with Eqs. (17), (20) and (21), we have:

$$\left(\mathrm{P}_F\widehat{\nabla}^2 - \frac{\partial}{\partial \widehat{\tau}}\right)\left[\left(1 + \frac{1}{\eta}\right)\widehat{\nabla}^2 w_D' - \widehat{\nabla}_P{}^2\theta'\right] + \mathrm{P}_F\mathrm{Q}_F\widehat{\nabla}^2\left(\frac{\partial^2 w_D'}{\partial \widehat{z}^2}\right) = 0. \tag{22}$$

It is supposed that the design of the convective signal is stationary for the deliberated problem. This statement is legal if the assessment of P_F is more than one as detected by Chandrasekhar [36]. Consequently, for the inspection of natural stable system, considering the normal mode as:

$$\begin{pmatrix} w_D', \\ \theta' \end{pmatrix} = \begin{bmatrix} W(\widehat{z}), \\ \Theta(\widehat{z}) \end{bmatrix} \exp\left[ia_x\widehat{x} + ia_y\widehat{y}\right] \tag{23}$$

Here, $\delta = \sqrt{a_x^2 + a_y^2}$ is overall plane wave number. Then, by using Eq. (23), Eq. (22) and Eq. (19) converted to two ordinary differential equations with boundary condition as:

$$\left[\left(1+\frac{1}{\eta}\right)\left(D^2-\delta^2\right)W+\delta^2\Theta\right]+Q_F D^2 W = 0, \tag{24}$$

$$\frac{R_I}{2}\left(2\hat{z}-\psi\right)W+\left(D^2-\delta^2\right)\Theta = 0 \tag{25}$$

Type (I) both boundaries isothermals
$$W = \Theta = 0 \quad \text{at } \hat{z} = 0,1 \tag{26a}$$

Type (II) lower insulated and upper isothermal
$$W = D\Theta = 0 \text{ at } \hat{z} = 0 \text{ and} \tag{26b}$$
$$W = \Theta = 0 \quad \text{at } \hat{z} = 1.$$

Here $D \equiv d/d\tilde{z}$.

4. Solution technique

The system of Eqs. (24) and (25) forms an eigenvalue problem and solved it by considering the Galerkin process. Consequently, the solutions of Eqs. (24) and (25) are taken as:

$$W = \sum_{p=1}^{S} A_p W_p, \quad \Theta = \sum_{p=1}^{S} B_p \Theta_p. \tag{27}$$

Here A_p and B_p are unidentified coefficients. Here, W_p and Θ_p accomplish the boundary conditional (Eq. (26)) and considered as:
Type (I) both boundaries isothermals:
$$W_p = \Theta_p = \sin\left(p\pi\hat{z}\right) \tag{28a}$$

Type (II) lower insulated and upper isothermal:
$$W_p = \sin\left(p\pi\hat{z}\right); \Theta_p = 1-\left(\hat{z}\right)^{p+1} \tag{28b}$$

Relating Eq. (27) into Eqs. (24) and (25) and sighted the orthogonal rule, the following system of algebraic equations is obtained:
$$C_{jp}A_p + D_{jp}B_p = 0, \tag{29}$$
$$E_{jp}A_p + F_{jp}B_p = 0.$$

Here, $\quad C_{jp} = \left\langle\left(1+\frac{1}{\eta}\right)\left(DW_j DW_p - \delta^2 W_j W_p\right)+Q_F DW_j DW_p\right\rangle,\quad D_{jp} = \left\langle\delta^2 W_j \Theta_p\right\rangle,$

$E_{jp} = \left\langle\frac{R_I}{2}\Theta_j W_p\left(2\hat{z}-\psi\right)\right\rangle$ and $F_{jp} = \left\langle D\Theta_j D\Theta_p - \delta^2 \Theta_j \Theta_p\right\rangle$. Here $\left\langle AB\right\rangle = \int\limits_0^1 AB d\hat{z}.$

The Eq. (29) makes an eigenvalue problem and resolved it by utilizing the "*eig*" function in Matlab. Here, the "*eig*" function is used with QZ algorithm to calculate the internal Rayleigh number R_I as an eigenvalue. The

estimations of $R_{I,c}$ and δ_c are found with the application of the golden search practice.

5. Results and discussion

5.1. Analytical result

For type (1) boundary conditions, the analytical results are derived by considering $S = 2$. Thus, from Eq. (29) for a non-trivial solution condition, the internal Rayleigh number R_I and the correspondent critical wave number δ_c are obtained as:

$$R_I = \frac{9\pi^2 \sqrt{\delta^2 + \pi^2} \sqrt{\delta^2 + 4\pi^2} \sqrt{\delta^2(1+\eta) + \pi^2(1+\eta+\eta Q_F)} \sqrt{\delta^2(1+\eta) + 4\pi^2(1+\eta+\eta Q_F)}}{16\delta^2\eta} \tag{30}$$

$$\delta_c = \sqrt{\frac{2\pi^2 \sqrt{1+\eta+\eta Q_F}}{\sqrt{1+\eta}}} \tag{31}$$

For type (II) boundary conditions, the analytical results are presented by taking $S = 1$. Thus, from Eq. (29), the internal Rayleigh number R_I and the correspondent critical wave number δ_c for type (II) boundary conditions, are derived as:

$$R_I = \frac{(5+2\delta^2)\pi^6 [\delta^2(1+\eta) + \pi^2(1+\eta+\eta Q_F)]}{45\delta^2\eta(4+\pi^2)} \tag{32}$$

$$\delta_c = \sqrt{\sqrt{\frac{5}{2}}\pi \left\{ \frac{\sqrt{1+\eta+\eta Q_F}}{\sqrt{1+\eta}} \right\}} \tag{33}$$

To estimate the impact of the Casson constraint η and the magnetic Chandrasekhar number Q_F on the onset of convective movement analytically, the behaviour of $\dfrac{\partial R_I}{\partial \eta}$ and $\dfrac{\partial R_I}{\partial Q_F}$ are examined. Now, Eq. (32) gives:

$$\frac{\partial R_I}{\partial \eta} = -\frac{(5+2\delta^2)\pi^6(\delta^2+\pi^2)}{45\delta^2\eta^2(4+\pi^2)} \tag{34}$$

$$\frac{\partial R_I}{\partial Q_F} = \frac{(5+2\delta^2)\pi^8}{45\delta^2(4+\pi^2)} \tag{35}$$

From Eqs. (34) and (35), it is establish that the Casson constraint η accelerates the onset of convective motion whereas, the magnetic Chandrasekhar number Q_F has the opposite impact on it.

5.2. Numerical result and discussion

For the studied problem, it is not feasible to get a precise analytical solution. Therefore, the higher-order (six-order) Galerkin process is also used to solve the consequential eigenvalue problem for diverse valuations of the Casson constraint η and the magnetic Chandrasekhar number Q_F.

Table 1. Assessment of the critical internal Rayleigh number $R_{I,c}$ and critical wave number δ_c with numerous levels of the Galerkin estimation S, the Casson constraint η and the magnetic Chandrasekhar number Q_F for type (1) both boundaries isothermals and for type (II) lower insulated and upper isothermal at $Q_F = 5$.

	S	$\eta = 1$		$\eta = 3$		$\eta = 5$		Regular fluid $(\eta \to \infty)$	
		$R_{I,c}$	δ_c	$R_{I,c}$	δ_c	$R_{I,c}$	δ_c	$R_{I,c}$	δ_c
Type (1)	2	2011.34	6.08	1636.27	6.56	1558.20	6.70	1438.167	6.95
	3	1923.74	6.38	1564.13	6.89	1489.25	7.04	1374.08	7.31
	4	1920.58	6.40	1561.46	6.91	1486.68	7.06	1371.66	7.33
	5	1920.38	6.40	1561.30	6.91	1486.52	7.06	1371.51	7.33
	6	1920.35	6.40	1561.27	6.91	1486.50	7.06	1371.49	7.33
Type (1I)	1	342.76	3.05	291.78	3.29	281.24	3.36	265.10	3.49
	2	292.18	3.65	243.65	4.04	233.48	4.15	217.77	4.37
	4	288.07	3.63	240.35	4.01	230.36	4.13	214.94	4.33
	5	288.06	3.63	240.35	4.01	230.35	4.13	214.93	4.33
	6	288.07	3.63	240.35	4.01	230.35	4.13	214.93	4.33

The convergence of the Galerkin technique with several terms of the Galerkin routine is offered in Table 1 with the variation of the Casson constraint η at $Q_F = 5$. From Table 1, it is distinguished that the analytical result presented by Eq. (30) with two terms Galerkin process has overall 5% error and the analytical result presented by Eq. (32) with single term Galerkin process has nearly overall 19% error. From Table 1, it is also established that overall one decimal place precision on the valuations of the critical internal Rayleigh $R_{I,c}$ obtained spending six terms of Galerkin technique. Therefore, the numerical results are presented here by taking the six terms Galerkin process.

To endorse the exactitude of the numerical route used in this analysis, first sample calculations are succeeded for the normal fluid with the nonattendance of magnetic force $(Q_F = 0, \ \eta \to \infty)$ and outcomes are connected with the outcomes provided by Nouri-Borujerdi et al. [37] in Table 2.

Table 2: Disparity of $R_{I,c}$ and δ_c with diverse values of Q_F and η for type (1) both boundaries isothermals.

Q_F	$\eta = 1$		$\eta = 3$		$\eta = 5$		Regular fluid $(\eta \to \infty)$	
	$R_{I,c}$	δ_c	$R_{I,c}$	δ_c	$R_{I,c}$	δ_c	$R_{I,c}$	δ_c
0	942.77	4.68	628.52	4.68	565.66	4.68	471.39 [37]	4.68 [37]
5	1920.35	6.40	1561.27	6.91	1486.50	7.06	1371.49	7.33
10	2742.98	7.33	2337.15	8.01	2250.96	8.20	2116.98	8.55
15	3505.73	8.01	3059.28	8.78	2963.40	9.00	2813.53	9.40
20	4233.97	8.55	3751.37	9.40	3646.97	9.64	3483.18	10.07
25	4939.01	9.00	4423.57	9.91	4311.48	10.17	4135.15	10.63
30	5627.06	9.40	5081.34	10.36	4962.18	10.63	4774.36	11.11

From the Table 2, it is recognized that the contract is marvellous and thus recommend the accurateness of the routine used in this paper. For the normal fluid and in the nonappearance of magnetic power $\left(Q_F = 0,\ \eta \to \infty\right)$, Table 2 shows $R_{I,c} = 471.39$ and $\delta_c = 4.68$. These are nearly same to the values detected by Nouri-Borujerdi et al. [37] $\left(R_{I,c} = 471.3846, \delta_c = 4.6751\right)$.
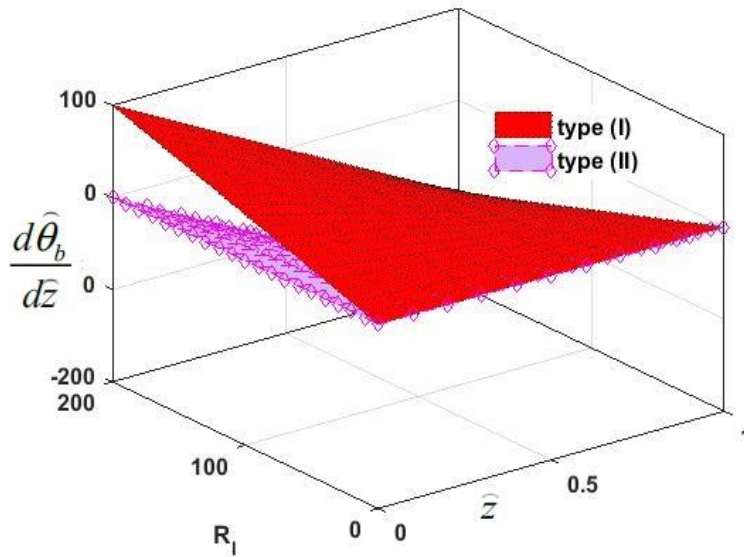

Fig. 2: Effect of internal Rayleigh number R_I on the distribution of basic temperature gradient $\dfrac{d\widehat{\theta}_b}{d\widehat{z}}$.

Fig. 2 displays the circulation of the basic temperature gradient $\dfrac{d\widehat{\theta}_b}{d\widehat{z}}$ under the impact of internal Rayleigh number R_I for both types of boundary conditions. From this graph, it is recognized that for type (I) boundary conditions, the convective wave concentrates (negative basic temperature gradient) in the upper layer if it arises, whereas for type (II) boundary conditions, it emphases in the whole layer. From Fig. 2, it is also found that the circulation of the basic temperature gradient increases with internal Rayleigh number R_I and therefore the system is less stable with increasing R_I.

Fig. 3 and Fig. 4 show the neutral plots for varied assessments of the magnetic Chandrasekhar number Q_F and the Casson constraint η, respectively. From these plots, it is distinguished that the neutral plots are analogous in a topological aptitude. This allows that the linear stability standard can be specified in state of the critical internal Rayleigh number $R_{I,c}$, smaller which the structure is stable and not-stable above. From these graph, it is also established that on rising the value of η, the assessment of R_I tends to decay, i.e., the arrangement pushes to destabilize, while Q_F has a stabilizing inspiration on the stability of the structure.

Fig. 5 (5a,b) and Fig. 6 (6a,b) show the distinctions of $R_{I,c}$ and δ_c with the magnetic Chandrasekhar number Q_F for several estimates of the Casson constraint η, respectively with both types of boundary surroundings. The imports are also disclosed in Table 2 for type (I) and Table 3 for type (II) boundary conditions. From Table 2, Table 3 and Fig. 5, it is recognized that the estimates of $R_{I,c}$ falls with the Casson constraint η while it upsurges with the magnetic Chandrasekhar number Q_F. This demonstrates that the stability of the arrangement upsurges with Q_F.
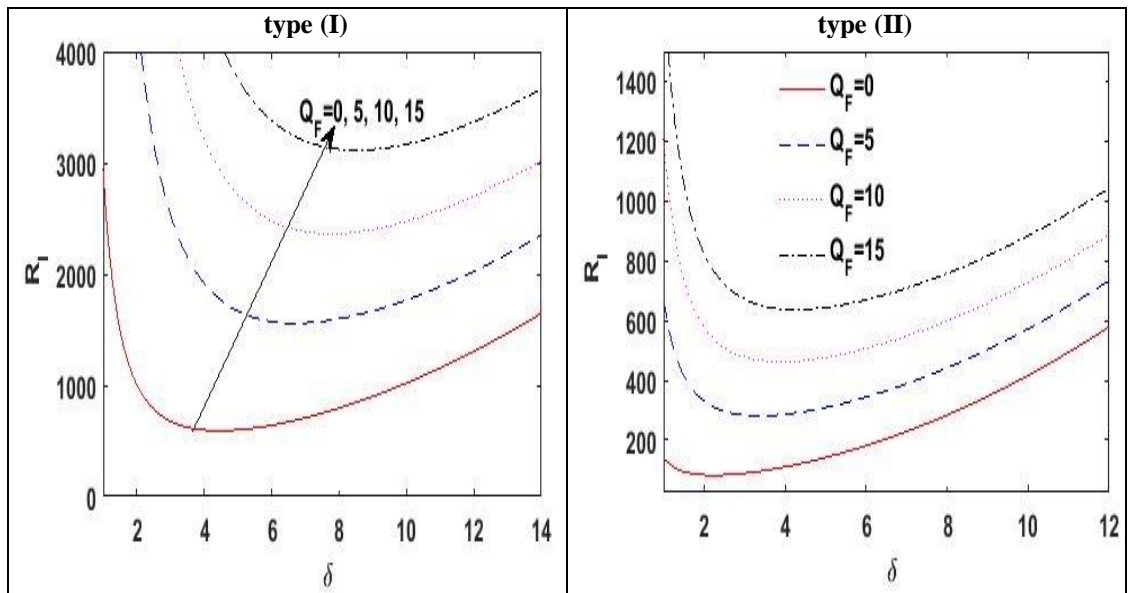
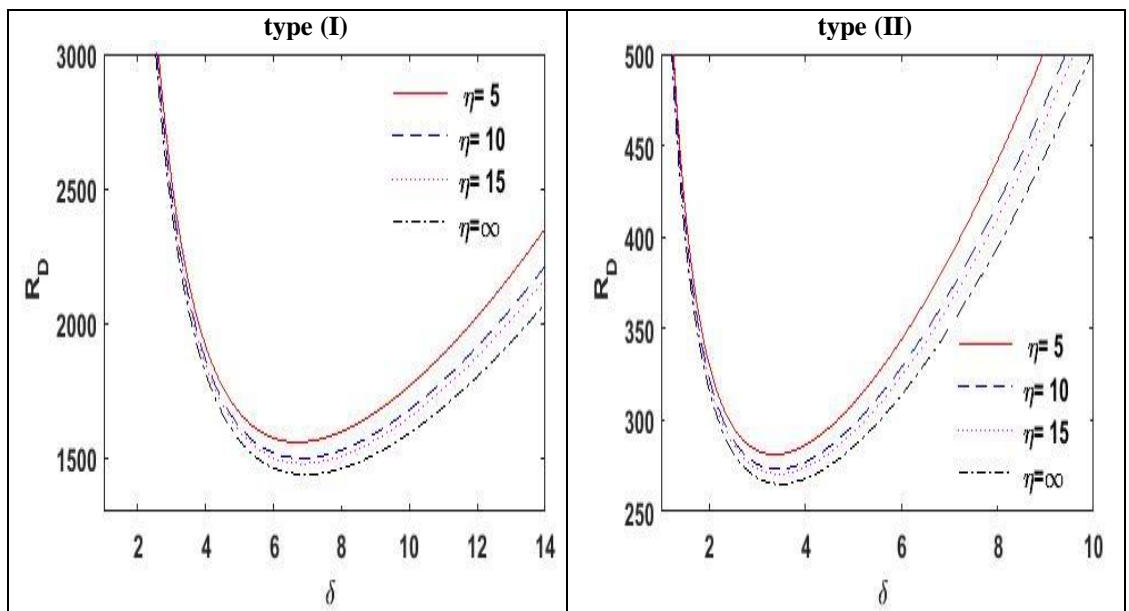**Fig. 3.** Neutral stability plots with disparity of Q_F at $\eta = 5$.

Fig. 4. Neutral stability plots with disparity of η at $Q_F = 5$.

The stabilizing control of Q_F on the arrangement is found because increasing Q_F increases the strength of Lorentz force, and the Lorentz force offers more fight for the transport of the Casson fluid flow. The destabilizing effect of η on the system is detected because raising the Casson constraint η reduces the yield stress of the Casson lequid; this creates the arrangement more unstable.

Table 3: Disparity of $R_{I,c}$ and δ_c with diverse values of Q_F and η for type (II) lower insulated and upper isothermal boundaries.

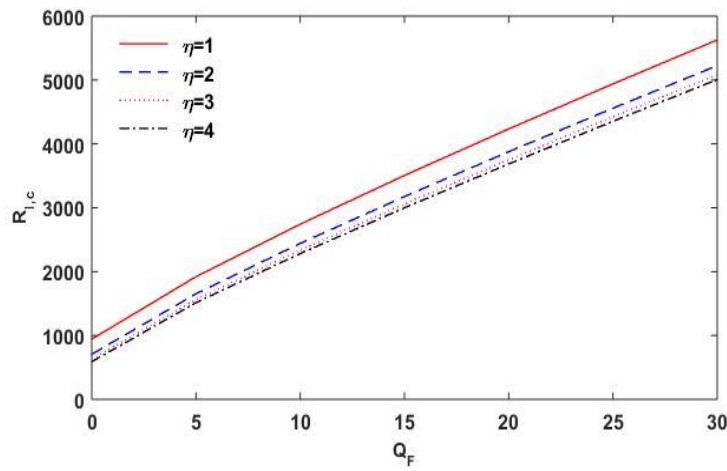| Q_F	$\eta = 1$		$\eta = 3$		$\eta = 5$		Regular fluid $(\eta \to \infty)$	
	$R_{I,c}$	δ_c	$R_{I,c}$	δ_c	$R_{I,c}$	δ_c	$R_{I,c}$	δ_c
0	123.73	2.45	82.49	2.45	74.24	2.45	61.87	2.45
5	288.07	3.63	240.35	4.01	230.35	4.13	214.93	4.33
10	429.87	4.33	375.02	4.85	363.28	4.99	344.94	5.26
15	562.53	4.85	501.42	5.44	488.18	5.60	467.39	5.90
20	689.87	5.26	623.19	5.90	608.63	6.08	585.70	6.41
25	813.63	5.60	741.89	6.29	726.16	6.48	701.31	6.83
30	934.78	5.90	858.38	6.63	841.57	6.83	814.96	7.19

Fig 5a: Result of Q_F on $R_{I,c}$ for diverse values of Casson constraint η for type (1) both boundaries isothermals.
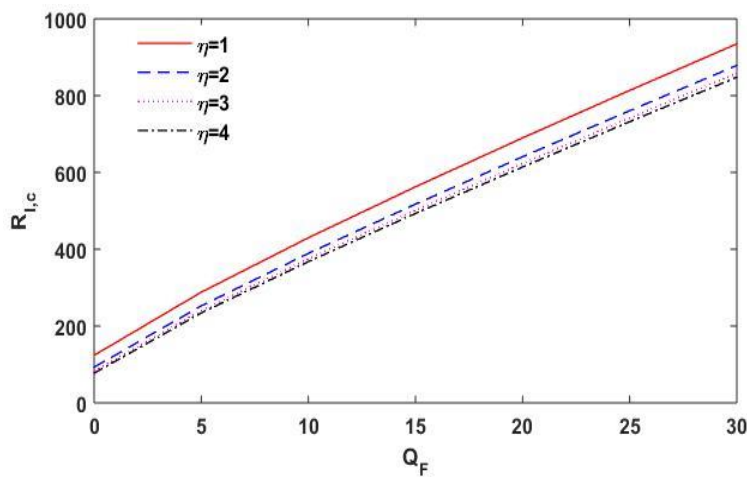

Fig 5b: Result of Q_F on $R_{I,c}$ for diverse values of Casson constraint η for type (II) lower insulated and higher isothermal boundaries.
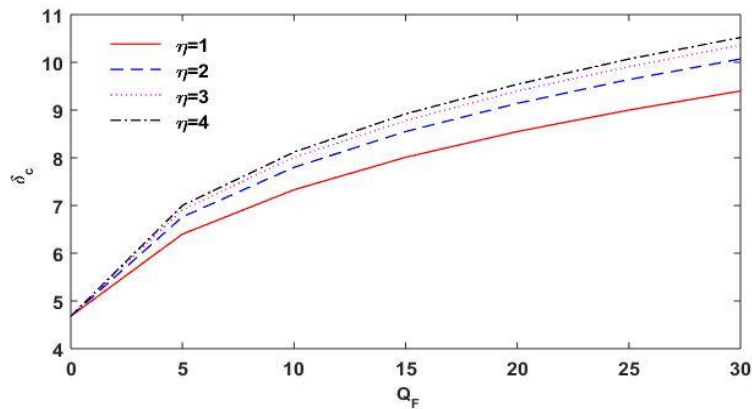
Fig 6a: Result of Q_F on δ_c for diverse values of Casson constraint η for type (1) both isothermal boundaries
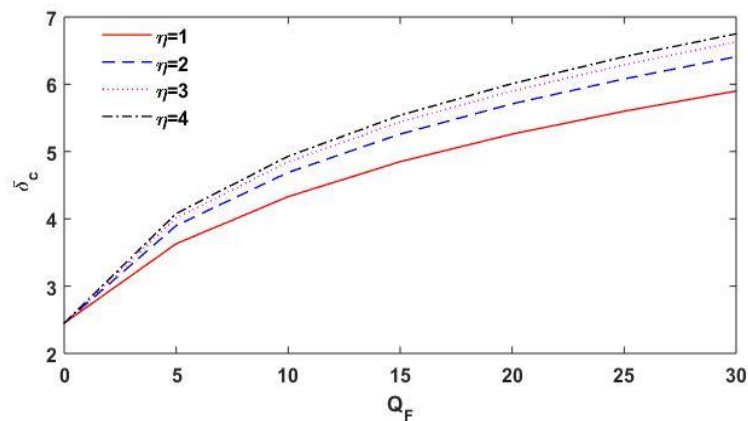

Fig 6b: Result of Q_F on δ_c for diverse values of Casson constraint η for type (II) lower insulated and higher isothermal boundaries.

From Fig. 6, it is noticed that the critical wave number δ_c surges with η and Q_F. This shows that the extent of the convective cells declines by increasing η and Q_F. Also, it is detected that in the nonappearance of magnetic power, the Casson constraint η has no impact on δ_c. From these plots, it is also predicted that the structure is more stable for type (I) boundary conditions for which both boundary planes are isothermal.

6. Conclusions

In this examination, the magnetic power significance on the arrival of Casson liquid convective drive in a permeable medium is evaluated analytically as well as numerically. Two types of thermal boundaries are measured, namely, type (I) both isothermal and type (II) lower insulated and top isothermal boundaries. The numerical treatment for the problem is presented correctly to one decimal place using six terms Galerkin process whereas, the analytical results are presented with one and two terms Galerkin process. The analytical result presented by the single term Galerkin process has nearly overall 19% error while, with two terms Galerkin process the error was overall 5%. Results indicated that for type (I) boundary conditions, the convective wave concentrates in the upper layer whereas, for type (II) boundary conditions it emphases in the whole layer, if it occurs. The Casson constraint η rushes the convective motion whereas; the magnetic Chandrasekhar number Q_F postpones it. The size of the convective cell declines with Q_F. The Casson constraint η has no impact on the size of the convective cell without magnetic force while in the incidence of magnetic force it drops the size of convective cells. The arrangement shows more stability for type (I) boundary conditions for which both boundary planes are isothermal.

References

[1]   A. Arslan, G. Fantuzzi, J. Craske, A. Wynn, Bounds on heat transport for convection driven by internal heating, *Journal of Fluid Mechanics,* Vol. 919, pp. A15, *2021.*

[2]   P. H. Roberts, Convection in horizontal layers with internal heat generation. Theory, *Journal of Fluid Mechanics,* Vol. 30, No. 1, pp. 33-49, 1967.

[3]   M. Tveitereid, Thermal convection in a horizontal porous layer with internal heat sources, *International Journal of Heat and Mass Transfer,* Vol. 20, No. 10, pp. 1045-1050, 1977/10/01/, 1977.

[4]   D. A. Nield, A. Bejan, 2006, *Convection in porous media*, Springer,

[5]   R. Gasser, M. Kazimi, Onset of convection in a porous medium with internal heat generation, *Journal of Heat Transfer,* Vol. 98, No. 1, pp. 49-54, 1976.

[6]   D. Yadav, J. Wang, J. Lee, Onset of Darcy-Brinkman convection in a rotating porous layer induced by purely internal heating, *Journal of Porous Media,* Vol. 20, No. 8, pp. 691-706, 2017.

[7]   D. Yadav, J. Lee, H. H. Cho, Brinkman convection induced by purely internal heating in a rotating porous medium layer saturated by a nanofluid, *Powder Technology,* Vol. 286, pp. 592-601, 2015.

[8]   A. Mahajan, Sunil, M. K. Sharma, Linear stability analysis of penetrative convection via internal heating in a ferrofluid saturated porous layer, *Fluids,* Vol. 2, No. 2, pp. 22, 2017.

[9]   D. Yadav, The Onset of Convective Activity in an Anisotropic Porous Medium Layer with Internal Heating and Inconsistent Gravity Effects, *Revista Cubana de Física,* Vol. 37, No. 1, pp. 24-33, 2020.

[10]   C. Jain, V. S. Solomatov, Onset of convection in internally heated fluids with strongly temperature-dependent viscosity, *Physics of Fluids,* Vol. 34, No. 9, pp. 096604, 2022.

[11]   P. Akbarzadeh, The onset of MHD nanofluid convection between a porous layer in the presence of purely internal heat source and chemical reaction, *Journal of Thermal Analysis and Calorimetry,* Vol. 131, No. 3, pp. 2657-2672, 2018/03/01, 2018.

[12]   F. Capone, M. Gentile, A. A. Hill, Penetrative convection via internal heating in anisotropic porous media, *Mechanics Research Communications,* Vol. 37, No. 5, pp. 441-444, 2010/07/01/, 2010.

[13]   S. N. Gaikwad, S. Kouser, Double diffusive convection in a couple stress fluid saturated porous layer with internal heat source, *International Journal of Heat and Mass Transfer,* Vol. 78, pp. 1254-1264, 2014/11/01/, 2014.

[14]   D. Nield, A. Kuznetsov, Onset of convection with internal heating in a porous medium saturated by a nanofluid, *Transport in porous media,* Vol. 99, No. 1, pp. 73-83, 2013.

[15]   F. Ali, N. A. Sheikh, I. Khan, M. Saqib, Solutions with Wright function for time fractional free convection flow of Casson fluid, *Arabian Journal for Science and Engineering,* Vol. 42, pp. 2565-2572, 2017.

[16]   T. Anwar, P. Kumam, W. Watthayu, Unsteady MHD natural convection flow of Casson fluid incorporating thermal radiative flux and heat injection/suction mechanism under variable wall conditions, *Scientific Reports,* Vol. 11, No. 1, pp. 4275, 2021/02/19, 2021.

[17]   M. Hamid, M. Usman, Z. H. Khan, R. Ahmad, W. Wang, Dual solutions and stability analysis of flow and heat transfer of Casson fluid over a stretching sheet, *Physics Letters A,* Vol. 383, No. 20, pp. 2400-2408, 2019/07/18/, 2019.

[18]   O. Makinde, M. Gnaneswara Reddy, MHD peristaltic slip flow of Casson fluid and heat transfer in channel filled with a porous medium, *Scientia Iranica,* Vol. 26, No. 4, pp. 2342-2355, 2019.

[19]   G. Rana, R. Chand, V. Sharma, On the onset of instability of a viscoelastic fluid saturating a porous medium in electrohydrodynamics, *Revista Cubana de Física,* Vol. 33, No. 2, pp. 89-94, 2016.

[20]   G. C. Rana, H. Saxena, P. K. Gautam, The Onset of Electrohydrodynamic Instability in a Couple-Stress Nano-fluid Saturating a Porous Medium: Brinkman Mode, *2019,* Vol. 36, No. 1, pp. 9, 2019-07-14, 2019.

[21]   M. S. Aghighi, A. Ammar, C. Metivier, M. Gharagozlu, Rayleigh-Bénard convection of Casson fluids, *International Journal of Thermal Sciences,* Vol. 127, pp. 79-90, 2018.

[22]   M. Devi, U. Gupta, S. Bandari, Internal heat source effects on thermosolutal convection of Casson nanofluids embedded by Darcy-Brinkman model, *Numerical Heat Transfer, Part B: Fundamentals*, pp. 1-16.

[23]   H. Qadan, H. Alkasasbeh, N. Yaseen, M. Z. Sawalmeh, S. ALKhalafat, A Theoretical Study of Steady MHD mixed convection heat transfer flow for a horizontal circular cylinder embedded in a micropolar Casson fluid with thermal radiation, *Journal of Computational Applied Mechanics,* Vol. 50, No. 1, pp. 165-173, 2019.

[24]   G. Reddy, R. Ragoju, S. Shekhar, Thermohaline convection of a Casson fluid in a porous layer: Linear and non-linear stability analyses, *Physics of Fluids,* Vol. 35, No. 9, 2023.

[25]   D. Yadav, S. B. Nair, M. K. Awasthi, R. Ragoju, K. Bhattacharyya, Linear and nonlinear investigations of the impact of chemical reaction on the thermohaline convection in a permeable layer saturated with Casson fluid, *Physics of Fluids,* Vol. 36, No. 1, 2024.

[26]   N. Rudraiah, D. Vortmeyer, Stability of finite-amplitude and overstable convection of a conducting fluid through fixed porous bed, *Wärme-und Stoffübertragung,* Vol. 11, No. 4, pp. 241-254, 1978.

[27]   M. B. Abd-el-Malek, M. M. Helal, Similarity solutions for magneto-forced-unsteady free convective laminar boundary-layer flow, *Journal of Computational and Applied Mathematics,* Vol. 218, No. 2, pp. 202-214, 2008/09/01/, 2008.

[28]   M. Devi, U. Gupta, Magneto-Convection in Casson Nanofluids with Three Different Boundaries, *Journal of Nanofluids,* Vol. 12, No. 5, pp. 1351-1359, 2023.

[29]   A. Mahajan, M. K. Sharma, The onset of convection in a magnetic nanofluid layer with variable gravity effects, *Applied Mathematics and Computation,* Vol. 339, pp. 622-635, 2018/12/15/, 2018.

[30]   M. Sheikholeslami, New computational approach for exergy and entropy analysis of nanofluid under the impact of Lorentz force through a porous media, *Computer Methods in Applied Mechanics and Engineering,* Vol. 344, pp. 319-333, 2019/02/01/, 2019.

[31]   N. Deepika, P. Murthy, P. Narayana, The Effect of Magnetic Field on the Stability of Double-Diffusive Convection in a Porous Layer with Horizontal Mass Throughflow, *Transport in Porous Media,* Vol. 134, No. 2, pp. 435-452, 2020.

[32]   J. C. Umavathi, M. A. Sheremet, O. Ojjela, G. J. Reddy, The onset of double-diffusive convection in a nanofluid saturated porous layer: Cross-diffusion effects, *European Journal of Mechanics - B/Fluids,* Vol. 65, pp. 70-87, 2017/09/01/, 2017.

[33]   M. Shuaib, M. Anas, H. u. Rehman, A. Khan, I. Khan, S. M. Eldin, Volumetric thermo-convective casson fluid flow over a nonlinear inclined extended surface, *Scientific Reports,* Vol. 13, No. 1, pp. 6324, 2023/04/18, 2023.

[34]   A. Khan, D. Khan, I. Khan, F. Ali, F. u. Karim, M. Imran, MHD Flow of Sodium Alginate-Based Casson Type Nanofluid Passing Through A Porous Medium With Newtonian Heating, *Scientific Reports,* Vol. 8, No. 1, pp. 8645, 2018/06/05, 2018.

[35]   H. Hamabata, M. Takashima, The effect of rotation on convective instability in a horizontal fluid layer with internal heat generation, *Journal of the Physical Society of Japan,* Vol. 52, No. 12, pp. 4145-4151, 1983.

[36]   S. Chandrasekhar, 2013, *Hydrodynamic and Hydromagnetic Stability*, Dover Publication,

[37]   A. Nouri-Borujerdi, A. R. Noghrehabadi, D. A. S. Rees, Influence of Darcy number on the onset of convection in a porous layer with a uniform heat source, *International Journal of Thermal Sciences,* Vol. 47, No. 8, pp. 1020-1025, 2008.